Relation between the solar wind dynamic pressure at Voyager 2 and the energetic particle events at Voyager 1

J. D. Richardson,[1,2] F. B. McDonald,[3] E. C. Stone,[4] C. Wang,[1,2] and J. Ashmall[1]

Received 29 March 2005; revised 11 May 2005; accepted 14 June 2005; published 29 September 2005.

[1] Starting in 2001, Voyager 1 observed three events characterized by enhanced fluxes of energetic particles. These events suggest that Voyager 1 made a close approach to, or a crossing of, the termination shock. Although the plasma experiment on Voyager 1 is not providing useful data, plasma data from Voyager 2 may shed light on the plasma conditions at Voyager 1. Before the first particle event, Voyagers 1 and 2 see similar particle signatures. Voyager 2 pressure and energetic particle flux profiles have similar structure. The merged interaction regions (MIRs) observed at Voyager 2 have counterparts in the Voyager 1 data. We propagate solar wind data from Voyager 2 to Voyager 1 and show that at the predicted MIR arrival times, there is always a response in the Voyager 1 particle data. These effects vary, from an increase in particle flux to a rapid turnoff of the particle event. We discuss the observed energetic particle effects and how the MIRs produce them.

Citation: Richardson, J. D., F. B. McDonald, E. C. Stone, C. Wang, and J. Ashmall (2005), Relation between the solar wind dynamic pressure at Voyager 2 and the energetic particle events at Voyager 1, *J. Geophys. Res.*, *110*, A09106, doi:10.1029/2005JA011156.

1. Introduction

[2] One of the most exciting recent events in heliospheric physics is the observation of intense energetic particle enhancements by Voyager 1 from roughly 90 to 95 AU [*Krimigis et al.*, 2003; *McDonald et al.*, 2003]. These events were first observed at Voyager 1 and have been identified as close as 75 AU from the Sun. Recent Voyager 2 data from outside 70 AU show events similar to the earliest ones observed by Voyager 1. The first large energetic particle event, termination shock precursor 1 (TSP1) lasted from mid-2002 to early 2003. The second (TSP2) started in mid 2003 and ended in late 2004, and the third (TSP3) started in early 2005. The particle intensities in these events increase by more than an order of magnitude over a wide range of energies [*McDonald et al.*, 2003; *Krimigis et al.*, 2003]. The TSP 1 and 2 particles flow along the azimuthal magnetic field from the direction where the field lines are connected to the Sun with anisotropies sometimes exceeding ten. The magnetic field did not increase significantly in the first two events nor did the magnetic field fluctuations [*Burlaga et al.*, 2003]. The plasma instrument on Voyager 1 is not functioning and cannot determine the solar wind speed. Speeds inferred from the Compton-Getting effect were initially reported to decrease from near 300 km/s outside these events to less than 50 km/s within these events [*Krimigis et al.*, 2003]. *Zhang* [2004], however, shows that use of a different background subtraction can yield Compton-Getting speeds consistent with a supersonic solar wind in these events. The ion spectra are power laws at low energies, but are still modulated at intermediate (anomalous cosmic ray) energies, and galactic electrons are observed for the first time [*McDonald et al.*, 2003]. These seemingly contradictory results led to the claim that Voyager 1 has crossed (and recrossed) the termination shock [*Krimigis et al.*, 2003] and the counterclaim that Voyager is seeing activity upstream of the shock [*McDonald et al.*, 2003; *Burlaga et al.*, 2003]. Recent work has suggested a solution to the outward streaming particle puzzle; if the termination shock is asymmetric and/or not circular, the field lines inside of Voyager 1 may be connected to the shock [*Jokipii et al.*, 2004]. Models of the termination shock suggest it is not circular [*Zank*, 1999] and recent inferences of the magnetic field direction in the local interstellar medium (LISM) would lead to a tilt of the heliosphere [*Lallement et al.*, 2005], so this hypothesis seems plausible.

[3] The termination shock position is determined by the balance of solar wind dynamic pressure and the pressure of the local interstellar medium (LISM). The solar wind dynamic pressure has variations on timescales of days to solar cycles, presumably faster than changes in the LISM, so the termination shock motion is largely driven by changes in the solar wind dynamic pressure [*Karmesin et al.*, 1995; *Wang and Belcher*, 1999]. Although the Voyager 1 plasma experiment (PLS) cannot determine the solar wind dynamic pressure, the solar cycle variation of

[1]Center for Space Research, Massachusetts Institute of Technology, Cambridge, Massachusetts, USA.
[2]Center for Space Science and Applied Research, Chinese Academy of Sciences, Beijing, China.
[3]Institute for Physical Science and Technology, University of Maryland, College Park, Maryland, USA.
[4]Division of Physics, Mathematics, and Astronomy, California Institute of Technology, Pasadena, California, USA.

Copyright 2005 by the American Geophysical Union.
0148-0227/05/2005JA011156

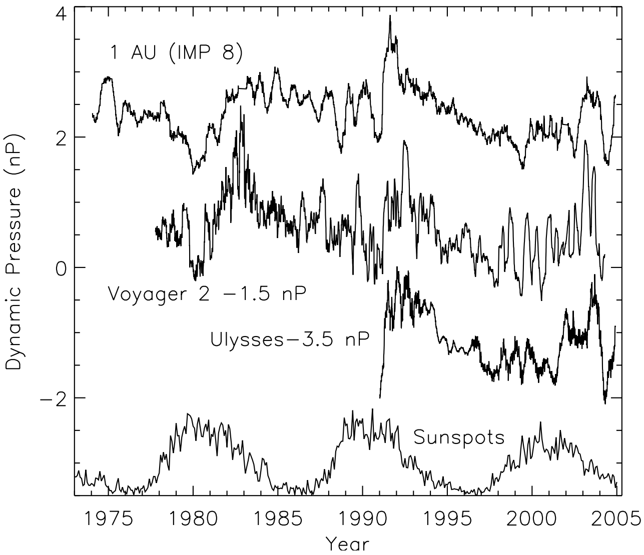

Figure 1. Plot of 51-day running averages of the solar wind dynamic pressures observed at 1 AU by IMP 8, by Ulysses (shifted by −3.5 nP), and by Voyager 2 (shifted by −1.5 nP), all time shifted to 1 AU. Ulysses and Voyager 2 pressures are normalized to 1 AU. The monthly average sunspot numbers are shown by the bottom trace. See color version of this figure in the HTML.

the solar wind dynamic pressure shows the same behavior at all heliolatitudes [*Richardson and Wang*, 1999], so we can use other spacecraft as proxies to identify large-scale pressure changes at Voyager 1. The PLS instrument on Voyager 2 is working well and Voyager 2 is now beyond 75 AU. Data from Voyager 2 are used to compare the timing of solar wind dynamic pressure changes with changes in the energetic particle fluxes associated with these events.

2. Pressure Comparisons

[4] Figure 1 shows 51-day running averages of the solar wind dynamic pressure observed at 1 AU by IMP 8, by Ulysses, and by Voyager 2. The data are time shifted to 1 AU using 51-day averages of the observed solar wind speed and normalized to 1 AU by multiplying by R^2. The monthly average sunspot number is at the bottom of the plot. The dynamic pressure varies with the solar cycle [*Lazarus and McNutt*, 1990]; the dynamic pressure is at a minimum near solar maximum, increases by roughly a factor of two over a few years, then slowly decreases until the next solar maximum. Data from all three spacecraft indicate that the pressure minimum for this solar cycle occurred near 2000; solar wind dynamic pressure increased to a maximum in 2003, and may now be decreasing. These changes take nearly a year to reach Voyager 1 from 1 AU. All the spacecraft see roughly the same pressure profiles despite their different latitude and longitude locations, thus we expect these pressure profiles to provide an accurate prediction of the dynamic pressure at Voyager 1.

[5] Since the same pressure profile occurs throughout the heliosphere, we can propagate the solar wind dynamic pressure observed by Voyager 2, which trails Voyager 1 by about 18.5 AU, ballistically outward to 90 AU using the observed solar wind speeds. The structure of the solar wind changes in 1999, at about 57 AU, to a regime dominated by large merged interaction regions (MIRs) [*Richardson et al.*, 2003]. Figure 2 shows that the dynamic pressure profile slowly decreases from 1999 to mid-2001 (with an intermediate minimum in early 2000), as is apparent in the 200-day average data. In mid-2001 the pressure starts to rise and reaches a peak in early 2004, after which the pressure decreases. The first energetic particle event begins near 2002.5, within twelve months of the end of the pressure minimum, when the termination shock should be near its minimum radial distance. The first TSP event ends in early 2003, then the second starts in mid-2003 during a time of increasing pressure, when the shock moves outward and is chased by Voyager. In early 2004, the shock should start to move inward toward Voyager, which could explain the change in character of the particle fluxes starting in 2005.

[6] Next we discuss the response of the energetic particle fluxes to changes in the solar wind pressure. To see if the energetic particle fluxes are affected by the pressure changes, we compare in Figure 3 the Voyager 2 energetic particle intensities to the solar wind parameters starting in 2001.6. At this time, the solar wind structure is dominated by MIRs. These MIRS are characterized by increased solar wind speeds, densities, pressures, and magnetic field strengths [*Richardson et al.*, 2003]. Figure 3 shows that the pressure increases at 2001.8, 2002.3, 2002.6, 2002.9, 2003.35, 2003.8, and 2004.3 are associated with energetic particle flux increases. The large energetic particle flux increase from 2003–2003.2 does not correspond to a pressure increase. All the MIRs affect the energetic particle profiles except for the one at 2004.7. Only one large particle

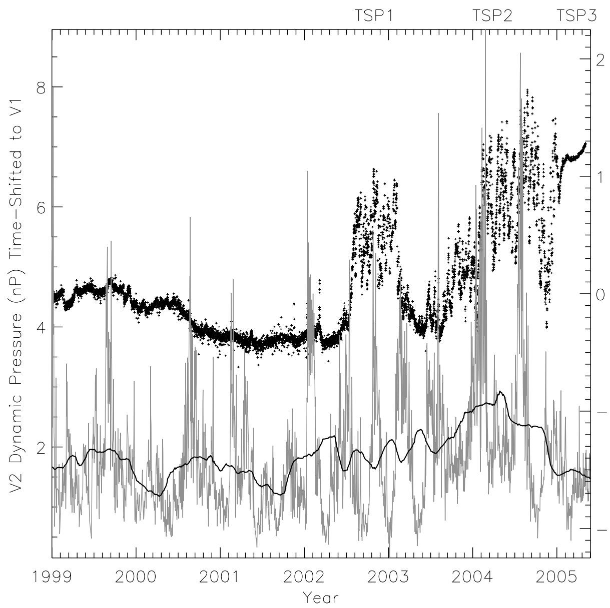

Figure 2. Daily averages of the solar wind dynamic pressures (jagged line), the CRS >0.5 MeV H counting rates (dotted line), and 200-day averages of the solar wind dynamic pressure (solid line) observed by Voyager 2. The data are time shifted to 90 AU using the observed solar wind speeds. See color version of this figure in the HTML.

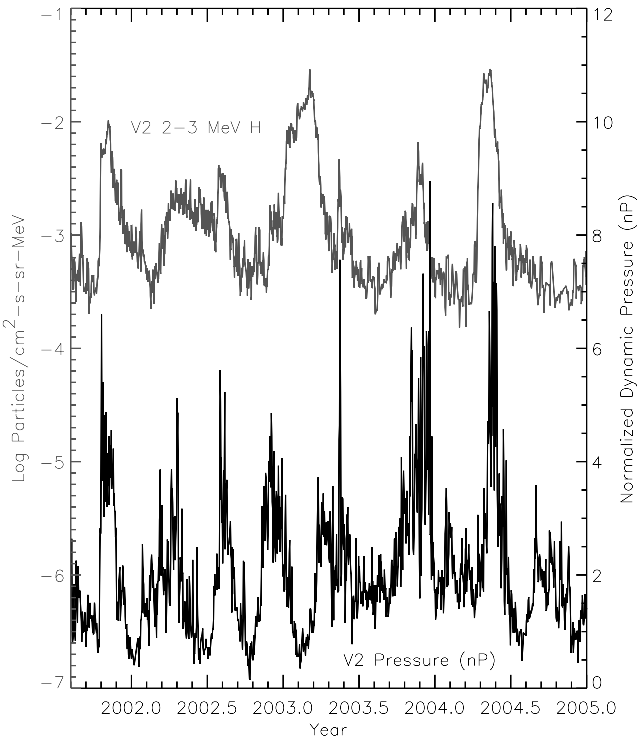

Figure 3. Comparison of the solar wind dynamic pressure (bottom line) and the 2–3 MeV H intensities (top line) measured at Voyager 2. See color version of this figure in the HTML.

increase out of 8 is not associated with a MIR. Since MIRs affect the Voyager 2 energetic particle fluxes, we expect they will also affect the Voyager 1 energetic particle fluxes.

[7] The next question is whether the energetic particle intensities at Voyager 1 and 2 are affected by the same events; that is, are the MIRs wide enough in longitudinal and latitudinal extent to have similar impacts at Voyager 1 and Voyager 2? Figure 4 compares the Voyager 1 and 2 cosmic ray subsystem (CRS) 2–3 MeV H intensities in the time period before the first energetic particle event. The Voyager 1 data are time shifted backwards 0.19 years to adjust for the solar wind propagation time. The large-scale features of the Voyager 1 and 2 energetic particle intensities generally track well, suggesting that solar wind events which affect energetic particles at Voyager 2 also affect energetic particles at Voyager 1 during this time period.

[8] These results suggest that we can use Voyager 2 solar wind dynamic pressures to study the changes in the energetic particle intensities observed by Voyager 1. Voyager 2 is the closest spacecraft to Voyager 1 in radial separation and on average is closest in heliolongitude (42°), although it is at about 25°S heliolatitude whereas Voyager 1 is at about 33°N heliolatitude. Most importantly, Voyager 2 is in the same region of the heliosphere as Voyager 1, a regime dominated by MIRs with large, in-phase variations of plasma speed, density, pressure, and magnetic field strength.

[9] We use 51-day averages of the observed Voyager 2 speeds to propagate the solar wind from Voyager 2 to Voyager 1. Since we are looking at small-scale structure, we need to be sure that this structure does not change significantly in the roughly 75 days the solar wind takes to go from Voyager 2 to Voyager 1. We compared the results of ballistic propagation to results from a one-dimensional, multifluid solar wind propagation model which includes pickup ions [*Wang and Richardson*, 2001]. The pressure predicted by ballistic propagation closely resembles that of the dynamic model, so ballistic propagation is a good approximation for pressure structures.

[10] We discuss two energetic particle populations in the following sections. The high-energy >70 MeV/nucleon particles are galactic cosmic rays; their intensities are modulated by global MIRs (GMIRs) and some pile up of flux may occur in front of a GMIR. The low-energy (few MeV) particles are accelerated either by the termination shock or the GMIR and these particles may be trapped by the GMIR.

[11] Figure 5 shows the Voyager 2 solar wind dynamic pressure and magnetic field strength from 2002–2005.3 propagated to the radial distance of Voyager 1. The bottom plot shows the >70 MeV/nucleon CRS counting rate and the Voyager 1 daily averages of the magnetic field strength. The Voyager 2 data are ballistically time shifted to Voyager 1 using 51-day averages of the observed Voyager 2 speed.

[12] The large MIRs which dominate solar wind dynamic pressure are apparent in the top plot. The top plot of Figure 5 shows increases of the Voyager 2 dynamic pressure and magnetic field strength at 2002.5, 2002.85, 2003.15, 2003.55, 2003.95, and 2004.55 (shifted times). An additional pressure peak is observed at 2004.9 but no magnetic field data are yet available at that time. The magnetic field enhancements at 2003.75 and 2003.85 (shifted times) do not have corresponding dynamic pressure increases, but neither do they cause decreases in the Voyager 2>70 MeV/nucleon CRS counting rate (not shown) and thus these increases may be local features.

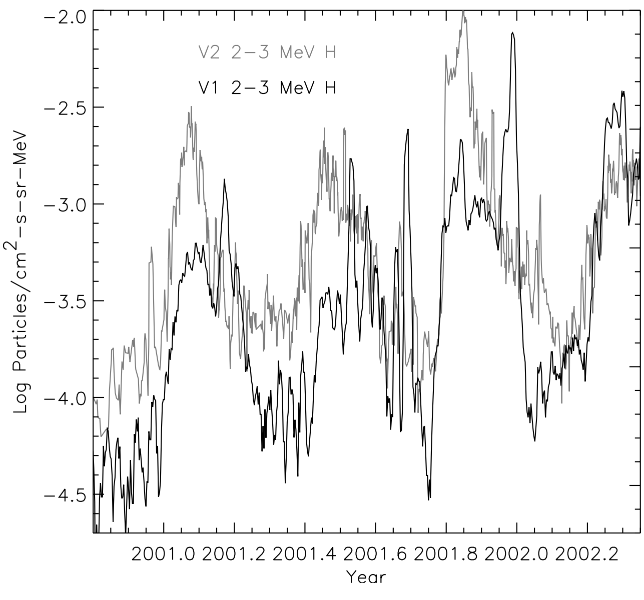

Figure 4. Comparison of the 2–3 MeV H intensities measured at Voyager 1 and 2; the Voyager 1 data are time shifted −0.19 years to account for the solar wind propagation time from Voyager 2 to Voyager 1. See color version of this figure in the HTML.

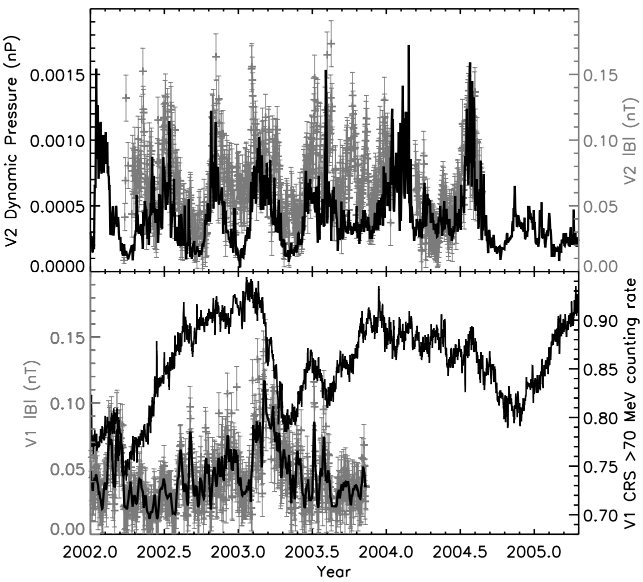

Figure 5. (top) Daily averages of the solar wind dynamic pressure observed by Voyager 2 propagated to the distance of Voyager 1 (black line) plotted with the Voyager 2 magnetic field magnitudes propagated to Voyager 1 (points with error bars). (bottom) Comparison of the Voyager 1 magnetic field magnitudes (points with error bars) to the Voyager 1>70 Mev/nucleon CRS counting rates (top line). The solid line shows 5-day running averages of *B*. See color version of this figure in the HTML.

[13] The Voyager 2 MIRs are not all present at Voyager 1. The bottom plot of Figure 5 shows that the peak in Voyager 2 pressure and magnetic field near 2002.45 (shifted time) is not seen in the Voyager 1 magnetic field data. These data are consistent with the >70 MeV/nucleon CRS data that serve as a proxy for magnetic field strength *B*: when *B* is above average the counting rate decreases and vice versa; this relation has held from 11 to 86 AU [*Burlaga et al.*, 1985, 2003]. The >70 MeV/nucleon counting rate does not decrease at 2002.45 (shifted time), suggesting that *B* is weaker than average. The Voyager 2 MIRs at 2002.85, 2003.15, 2003.55 2004.1, and 2004.55, and 2004.9 (shifted times) are associated with increases in magnetic field and/or decreases in the >70 MeV/nucleon counting rate observed at Voyager 1, so these five MIRs may be present at Voyager 1. Magnetic field data corresponding to the Voyager 2 MIR at 2004.1 are not yet available, but a decrease in the >70 MeV/nucleon counting rate coincides with the start of the Voyager 2 MIR at 2003.95.

[14] Figure 6 shows the connection between the MIRs observed by Voyager 2 (and propagated to the distance of Voyager 1) and the >0.5 MeV/nucleon H counting rate. The predicted arrival times at Voyager 1 of all the MIRs observed by Voyager 2 are associated with changes in the particle counting rates. We number the MIRs in Figure 6 to make the description of the phenomenology easier. The start of TSP1 is at the end of MIR 1; since Figure 5 shows that this MIR may not extend to Voyager 1, this connection may be fortuitous. MIR 2 coincides with an increase in the energetic particle counting rates. The energetic particle counting rate first increases with the arrival of MIR 3, then drops sharply as TSP1 ends. MIR 4 arrives at the same time as the start of TSP2; as the pressure decreases after the passage of MIR 4 the energetic particle counting rate increases. The arrival of MIR 5 occurs simultaneously with a very brief dropout of the energetic particle counting rate, followed by a step-like increase in the counting rate. MIR 6 similarly is associated with an increase in the energetic particle counting rate. The start of MIR 7 occurs at the same time as the end of TSP2. TSP3 starts in the middle of MIR 7. Thus all the MIRs seen at Voyager 2 seem to affect the energetic particle counting rate.

3. Discussion

[15] The mechanism for producing the energetic particle events is not well established, but is generally thought to result from connection of the magnetic field lines at Voyager to the termination shock. This connection could occur if Voyager were on either side of the shock, but in either case this connection must persist over the lengths of the TSP events, 6 months for the first and almost 1.5 years for the second.

[16] The pressure pulses shown in Figure 5 can significantly affect the shock position; *Wang and Belcher* [1999] show that sinusoidal, factor-of-two changes in the solar wind dynamic pressure over timescales of 180 days produce a 3 AU oscillation in the termination shock distance. The factor of ten changes in pressure which were observed could give even larger termination shock motions. These shock motions should be much faster than the motion of Voyager 1 and could lead to multiple shock approaches/crossings.

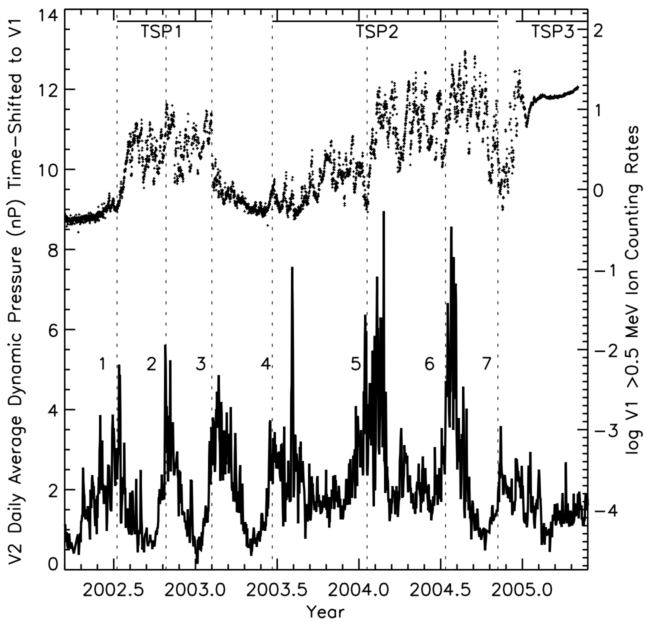

Figure 6. Daily averages of the solar wind dynamic pressure observed by Voyager 2 propagated to the distance of Voyager 1 (solid line) compared with 6-hour averages of the CRS >0.5 MeV/nucleon counting rates (dots). The onset of the MIRs is indicated by the vertical dashed lines, and the MIRs are numbered in order of occurrence. The TSP events are labeled at the top of the plot. See color version of this figure in the HTML.

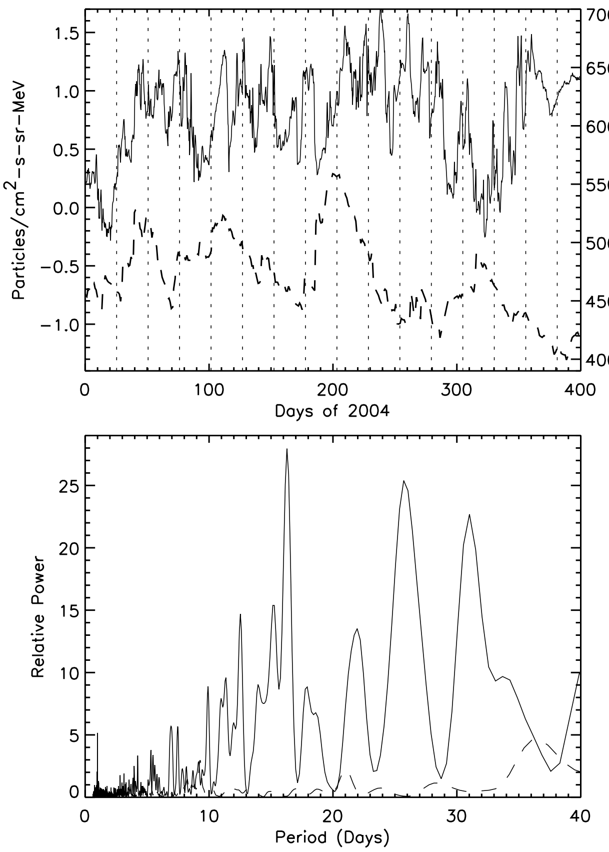

Figure 7. Daily averages of the solar wind speed observed by Voyager 2 propagated to the distance of Voyager 1 (bottom line) and 6-hour averages of the CRS >0.5 MeV/nucleon counting rates (top line). The vertical dotted lines are one soar rotation apart. The bottom plot shows Lomb-Scargill periodograms for these two data sets (the red line shows the speeds, and the black line shows the CRS counting rates). See color version of this figure in the HTML.

Zank and Mueller [2003] show that GMIRs can drive the termination shock out several AU and that the relaxation time is almost a year. Thus a simple relation between pressure changes and termination shock position might not exist if the recovery time of the termination shock were longer than the time between MIRs.

[17] The correlation of MIRs with energetic particle intensity changes is complicated since MIRs are regions of enhanced magnetic field as well as enhanced density and pressure. The magnetic field is enhanced in the MIRs in 2002 and 2003 and a multifluid MHD model predicts that all the MIRs have both enhanced pressure and magnetic field [*Richardson et al.*, 2003]. Strong magnetic field regions present a barrier for the inward transport of cosmic rays, so >70 MeV/nucleon intensities often decrease after a MIR passage. Energetic particle intensities sometimes increase before a MIR as the particles pile up ahead of the enhanced magnetic field region [*McDonald et al.*, 2000]. Changes in the magnetic field direction associated with the MIRs could alter the connection to the termination shock and thus the particle fluxes at Voyager 1.

[18] Figure 6 shows that the MIRs observed at Voyager 2 are all associated with changes in the energetic particle flux. We first discuss the associations we best understand, assuming the termination shock is still beyond Voyager 1. Increases in the dynamic pressure of the solar wind can drive the termination shock outward, resulting in disconnection of the magnetic field lines threading through Voyager 1 from the termination shock and a cessation of the particle flux along these field lines. The end of TSP1 and TSP2 coincide with the arrival of MIRs 3 and 7, respectively, and outward termination shock motion seems the likely cause. MIR 4 is also associated with a brief dropout of energetic particles, perhaps from the same effect. MIRs 2, 3 (before TSP1 ends), 4, 5, and 6 are all associated with increases in the particle flux which persist from days to months. MIRs 2 and 3 produce short-duration increases in the counting rates which are consistent with particles being trapped in the increased magnetic field in front of the MIRs. MIRs 4, 5, and 6 all occur at step increases in the energetic particle counting rates which last for months. We have no explanation for these long-term enhancements triggered by MIR passages, although it is possible that changes in the magnetic field direction across the MIRs change the connection to the termination shock.

[19] The other features of note are the short-scale fluctuations in the energetic particle counting rates. Semiperiodic spikes in the energetic particles flux were precursors of TSP1. These semiperiodic increases continue throughout the TSP events. Figure 7 shows the >0.5 MeV counting rate, the solar wind speed, and Lomb-Scargill periodograms [*Press et al.*, 1992, and references therein] for the observations in the top plot. The vertical dashed lines are spaced once per 25.4 day solar rotation. The energetic particle peaks are clearly not related to the plasma speed. The periodogram shows that they have the most power at about 16 and 26 days. The second period is the solar rotation rate. If we look at the power in the plasma speed we see no power at these periods; the same holds true for the other plasma parameters (not shown). Thus plasma fluctuations

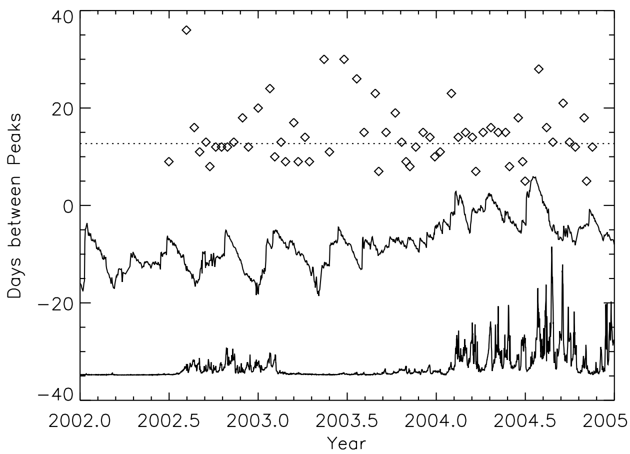

Figure 8. Time between peaks in the >0.5 MeV counting rate (diamonds) plotted with the >0.5 MeV counting rate (bottom line) and plasma speed (top line) profiles. The dashed lines are at 12.5-day intervals. See color version of this figure in the HTML.

are not the cause of these variations; changes in the magnetic field, in particular crossings of the current sheet, may be responsible. We have gone through the >0.5 MeV CRS data from the start of TSP2 to the present and picked out peaks. The spacing between those peaks versus time is shown in Figure 8. The solar wind speed and the >0.5 MeV CRS counting rates are also shown. The times between peaks are clustered about the 12.5 day, 1/2 solar rotation, dashed horizontal line in Figure 8. The spread is larger in the time period between TSP1 and TSP2, perhaps because some peaks are missed because of the low counting rates. Otherwise, the peak spacing seems to depend on neither the plasma speed nor the energetic particle flux. One might expect that if current sheet crossings were affecting the energetic particles fluxes, then the spacing would be larger when the solar wind was slowing and faster when the solar wind was speeding up. However, the only period with a long-term solar wind speed trend, the increase in speed from 2003.5 to 2004.1, does not have peak separations significantly shorter than during other time periods.

4. Summary

[20] The Voyager 2 solar wind dynamic pressures are propagated to Voyager 1 and show variations which coincide with some of the energetic particles structure observed by Voyager 1. TSP1 occurs about six months after the minimum in solar wind pressure; the pressure then increased until late 2004 and is now decreasing, so the termination shock should be moving toward the Voyager spacecraft. The solar wind structure in the outer heliosphere during and after solar maximum is dominated by large, semiperiodic MIRs. At Voyager 2 the solar wind pressure and the energetic particles flux are often correlated. The Voyager 1 and 2 energetic particle counting rates show similar structure. Thus we expect that MIRs observed at Voyager 2 will affect the energetic particle counting rates at Voyager 1. We find that most of the major changes in the energetic particles profile coincide with times that MIRs observed by Voyager 2 should reach Voyager 1. The effect vary; in three cases the energetic particles flux decreases and/or the TSP event ends, consistent with the termination shock being pushed outward. In two cases the energetic particles flux is briefly enhanced, consistent with energetic particles being trapped ahead of the high magnetic field region of the MIR. In three cases, the MIR passage coincides with a long-lived step increase in the energetic particle counting rates; but we do not understand those events.

[21] **Acknowledgments.** We thank N. Ness and L. Burlaga for use of the Voyager magnetic field data and for helpful discussion. We acknowledge the use of Ulysses SWOOPS data from the NSSDC (D. McComas, principal investigator). The work at MIT was supported under NASA contract 959203 from JPL to MIT and NASA grant NAG5-11623. C. Wang was supported in part by NNSFC 40204009 and 40325010 from China. This work was also supported in part by an international collaboration team grant from the Chinese Academy of Sciences.

[22] Shadia Rifai Habbal thanks Zdenek Nemecek and another referee for their assistance in evaluating this paper.

References

Burlaga, L. F., F. B. McDonald, M. L. Goldstein, and A. J. Lazarus (1985), Cosmic ray modulation and turbulent interaction regions near 11 AU, *J. Geophys. Res.*, *90*, 12,027–12,039.

Burlaga, L. F., N. F. Ness, E. C. Stone, F. B. McDonald, M. H. Acuna, R. P. Lepping, and J. E. P. Connerney (2003), Search for the heliosheath with Voyager 1 magnetic field measurements, *Geophys. Res. Lett.*, *30*(20), 2072, doi:10.1029/2003GL018291.

Jokipii, J. R., J. Giacalone, and J. Kota (2004), Transverse streaming anisotropies of charged particles accelerated at the solar wind termination shock, *Astrophys. J.*, *611*, L141, doi:10.1086/423993.

Karmesin, S. R., P. C. Liewer, and J. U. Brackbill (1995), Motion of the termination shock in response to an 11 year variation in the solar wind, *Geophys. Res. Lett.*, *22*, 1153–1156.

Krimigis, S. M., R. B. Decker, M. E. Hill, T. P. Armstrong, G. Gloeckler, D. C. Hamilton, L. J. Lanzerotti, and E. C. Roelof (2003), Voyager 1 exited the solar wind at a distance of 85 AU from the Sun, *Nature*, *426*, 45–48.

Lallement, R., E. Quemerais, J. L. Bertaux, S. Ferron, D. Koutroumpa, and R. Pellinen (2005), Deflection of the interstellar neutral hydrogen flow across the heliospheric interface, *Science*, *307*, 1447–1449.

Lazarus, A. J. and R. L. McNutt Jr. (1990), Plasma observations in the distant heliosphere: A view from Voyager, in *Physics of the Outer Heliosphere*, edited by S. Grzedzielski and D. E. Page, pp. 229–234, Elsevier, New York.

McDonald, F. B., L. F. Burlaga, R. E. McGuire, and N. F. Ness (2000), The onset of long-term cosmic ray modulation in cycle 23 coupled with a transient increase of anomalous cosmic rays in the distant heliosphere, *J. Geophys. Res.*, *105*, 20,997–21,004.

McDonald, F. B., A. C. Cummings, E. C. Stone, B. Heikkila, N. Lal, and W. R. Webber (2003), Enhancements of energetic particles near the heliospheric termination shock, *Nature*, *426*, 48–51.

Press, W. H., S. A. Teukolsky, W. T. Vetterling, and B. P. Flannery (1992), *Numerical Recipes in FORTRAN: The Art of Scientific Computing*, pp. 569–577, Cambridge Univ. Press, New York.

Richardson, J. D., and C. Wang (1999), The global nature of solar cycle variations of the solar wind dynamic pressure, *Geophys. Res. Lett.*, *26*, 561–564.

Richardson, J. D., C. Wang, and L. F. Burlaga (2003), Correlated solar wind speed, density, and magnetic field changes at Voyager 2, *Geophys. Res. Lett.*, *30*(23), 2207, doi:10.1029/2003GL018253.

Wang, C., and J. W. Belcher (1999), The heliospheric boundary response to large-scale solar wind fluctuations: A gas dynamic model with pickup ions, *J. Geophys. Res.*, *104*, 549–556.

Wang, C., and J. D. Richardson (2001), Energy partition between solar wind protons and pickup ions in the distant heliosphere: A three-fluid approach, *J. Geophys. Res.*, *106*, 29,401–29,408.

Zank, G. P. (1999), Interaction of the solar wind with the local interstellar medium: A theoretical perspective, *Space Sci. Rev.*, *89*, 413–688.

Zank, G. P., and H.-R. Mueller (2003), The dynamical heliosphere, *J. Geophys. Res.*, *108*(A6), 1240, doi:10.1029/2002JA009689.

Zhang, M. (2004), Uncertainties of solar wind speed determination using Voyager energetic particle anisotropy measurements at 85 AU, *Eos Trans. AGU*, *85*(47), Fall Meet. Suppl., Abstract SH41B-06.

J. Ashmall, Center for Space Research, Massachusetts Institute of Technology, 37-675, Cambridge, MA 02139, USA. (ja@space.mit.edu)

F. B. McDonald, Institute for Physical Science and Technology, University of Maryland, College Park, MD 20742-2431, USA. (fm27@umail.umd.edu)

J. D. Richardson, Center for Space Research, Massachusetts Institute of Technology, 37-655, Cambridge, MA 02139, USA. (jdr@space.mit.edu)

E. C. Stone, Division of Physics, Mathematics, and Astronomy, California Institute of Technology, Pasadena, CA 91125, USA. (ecs@srl.caltech.edu)

C. Wang, Center for Space Science and Applied Research, Chinese Academy of Sciences, P.O. Box 8701, Beijing 100080, China. (cw@space.mit.edu)